Extended Abstracts of the 2006 International Conference on Solid State Devices and Materials, Yokohama, 2006, pp. 554-555

P-4-1

Technology of Ferroelectric Thin Film Formation with Large Coercive Field for Future Scaling Down of Ferroelectric Gate FET Memory Device

Ichirou Takahashi, Tatsunori Isogai[1], Keita Azumi, Masaki Hirayama, Akinobu Teramoto, Shigetoshi Sugawa[1], and Tadahiro Ohmi
Phone: +81-22-795-3977 Fax: +81-22-795-3986 e-mail: ichirou@fff.niche.tohoku.ac.jp
New Industry Creation Hatchery Center, Tohoku University, Sendai 980-8579, Japan
[1]Graduate School of Engineering, Tohoku University, Sendai 980-8579, Japan

1. Introduction

Recently, $Sr_2(Ta_{1-x},Nb_x)_2O_7$ (STN) has attracted considerable attention as one of the most practical candidates for one-transistor-type ferroelectric memory devices because it is a bismuth- and lead-free ferroelectric material having a low dielectric constant [1]. Although in the application of MF(M)IS-FET-type memories, the most important problem is an improvement in data retention characteristic. On the other hand, it is indispensable to thin a ferroelectric film from the viewpoint of the scaling down of the device. For instance, when the coercive fields of the ferroelectric film of 50 nm thickness are 25 and 50 kV/cm, the obtained memory windows are only 0.25 and 0.5 V, respectively. To achieve the scaling down of the device, the technology that forms the thin ferroelectric film with a large coercive field is indispensable. Furthermore, development of new material that has a large coercive field is important.

In this work, we report the newly developed 100 nm $Sr(Ta_{0.7},Nb_{0.3})_2O_6$ film formed by ferroelectric multilayer stack (FMLS [2]) deposition. A memory window of 1.8V is obtained in the MFIS structure device with only 100 nm ferroelectric film for the first time. We also report the perovskite STN formation technology on SiO_2 by ion-bombardment-energy-assisted sputtering method and we have clarified the relationship between a ferroelectric crystal phase on amorphous SiO_2 and rf-sputtering plasma parameters such as ion bombardment energy.

2. Experimental

Figure 1 shows a modified rf-sputtering system for ferroelectric deposition. The detail of rf-sputtering condition is shown in Table. I . Oxygen radical treatment was performed by the microwave-excited (2.45 GHz) high-density ($> 10^{12}$ cm^{-3}) low-electron-temperature (< 1 eV) Kr/O_2 plasma system [2]. Characteristic of rf-sputtering plasma such as ion bombardment energy was measured by the single probe. The FMLS-MFIS structure device with newly developed $Sr(Ta_{0.7},Nb_{0.3})_2O_6$ (100nm, repeating 3.3 nm sputtering deposition and oxygen radical treatment 33 times) was fabricated, as shown in Fig. 2.

3. Results and Discussions

Figure 3 shows XRD patterns of the obtained film formed by FMLS process and this indicates that $Sr(Ta_{0.7},Nb_{0.3})_2O_6$ is formed well. Figure 4 and 5 show C-V characteristics of the device and the memory windows as function of writing operation voltage, respectively. The result indicates that a memory window of 1.5 V is obtained under 5 V operation for the first time in the MFIS structure device with only 100 nm ferroelectric. Maximum memory window is 1.8 V and this value is equivalent to a coercive field of 90 kV/cm. Figure 6(a) shows the device structure image and the process flow of IrO_2/STN(150 nm)/SiO_2/Si for ion-bombardment- energy-assisted sputtering experiment. In the case of the condition that rf power (R_I) and working pressure (P_W) are 14 W and 4 Pa, respectively, the XRD pattern corresponds to that of $Sr_3(Ta_{0.7},Nb_{0.3})_6Si_4O_{26}$, as shown in Fig. 7(a). In order to suppress the reaction between metal element and Si, we tried to provide ion-bombardment-energy to the surface of the film during STN sputtering deposition by increasing rf power and working pressure. Figure 8 shows the mapping of the STN deposition rate of 11 Å/min on the rf power–working pressure chart (R_I-P_W chart). The deposition rate is made constant in order to make migration time of ferroelectric element constant. At an (R_I, P_W) of (18 W, 20 Pa), the XRD patterns show that $Sr(Ta_{0.7},Nb_{0.3})O_3$ phase is obtained, as shown in fig. 7(b). This indicates that it is effective to provide large ion-bombardment-energy to the surface of the film to suppress the reaction between ferroelectric metal element and Si. However, it is difficult to form perovskite $Sr_2(Ta_{0.7},Nb_{0.3})_2O_7$ phase. $2Sr(Ta_{0.7},Nb_{0.3})O_3$ is composed of Sr_2O_2 and $(Ta_{0.7},Nb_{0.3})_2O_4$. This indicates that Ta and Nb are not oxidized up to pentad and oxygen vacancy exists. In order to obtain perovskite STN, 140 nm STN was formed on the 10 nm STN seed layer formed by oxygen radical treatment, as shown in Fig. 6(b). At an (R_I, P_W) of (14 W, 4 Pa), the XRD patterns indicate that $Sr_3(Ta_{0.7},Nb_{0.3})_6Si_4O_{26}$ and perovskite $Sr_2(Ta_{0.7},Nb_{0.3})_2O_7$ are fabricated, as shown in fig. 9(a). On the other hand, at an (R_I, P_W) of (18 W, 20 Pa), perovskite STN is fabricated, as shown in fig. 9(b). These results are summarized as the fabricated film phase mapping on the R_I-R_W chart, as shown in fig. 10. Figure 11 shows plasma potential, substrate voltage, and Kr^+ ion-bombardment-energy as function of rf power. This result indicates that, in order to obtain only perovskite STN phase, the ion-bombardment-energy of 24 eV or more must be provided to the surface of the film. Figure 12 shows C-V characteristics of IrO_2/STN (140 nm)/STN seed layer (10 nm)/SiO_2/Si device at an (R_I, P_W) of (18 W, 20 Pa). The device shows square hysteresis curves and a memory window of 1.65V under 8V writing operation. This value is equivalent to a coercive field of 55 kV/cm.

4. Conclusion

We have newly developed 100nm $Sr(Ta_{0.7},Nb_{0.3})_2O_6$ film by FMLS deposition. A memory window of 1.8V is obtained in the MFIS structure device with only 100 nm ferroelectric film for the first time. We have successfully developed the technology that forms perovskite STN with large coercive field on amorphous SiO_2 by ion-bombardment-energy-assisted sputtering method. An ion-bombardment-energy of 24 eV or more must be provided to the surface of the film to obtain only perovskite STN phase. The fabricated MFIS structure device shows square hysteresis curves, and a memory window of 1.65 V is obtained. These technologies can contribute to the scaling down of ferroelectric gate FET memory devices.

References

[1] Y. Fujimori et al., Jpn. J. Appl. Phys., vol. 38, p. 2285 (1999)
[2] I. Takahashi et al., Jpn. J. Appl. Phys., vol. 45, p. 3207 (2006)

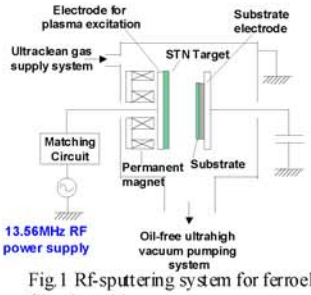

Fig.1 Rf-sputtering system for ferroelectric film deposition.

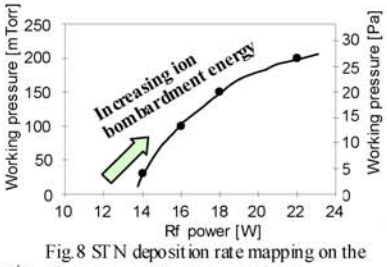

Fig.8 STN deposition rate mapping on the rf power–working pressure chart. The deposition rate is 11 Å/min.

Table Ⅰ. Sputtering conditions of ferroelectric film deposition.

	$Sr(Ta_{0.7},Nb_{0.3})_2O_6$	$Sr_2(Ta_{0.7},Nb_{0.3})_2O_7$	
	basic condition	basic condition (seed layer)	Plasma dependency
Gas	Kr/O_2	Kr/O_2	Kr/O_2
Rf frequency (MHz)	13.56	13.56	13.56
Rf power (W): [R_f] Working pressure (Pa): [P_W] (R_f, P_W)	(14, 4.0)	(14, 4.0)	**(14, 4.0) (16, 13.3) (18, 20.0) (22, 26.7)**
The ratio of O_2 partial pressure to total working pressure (%)	6	6	6
Substrate voltage	Floating	Floating	Floating
Substrate temperature	R.T.	R.T.	R.T.

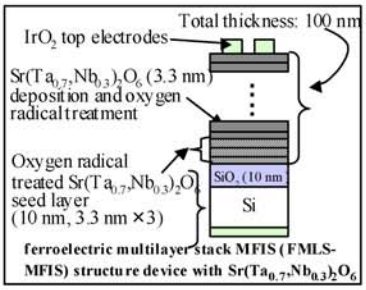

Fig.2 Device structure image of FMLS-MFIS structure device with $Sr(Ta_{0.7},Nb_{0.3})_2O_6$.

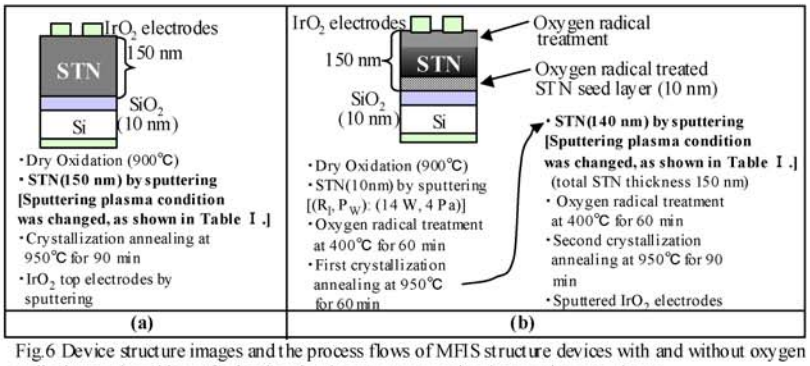

Fig.6 Device structure images and the process flows of MFIS structure devices with and without oxygen radical treated seed layer for ion-bombardment-energy-assisted sputtering experiment.

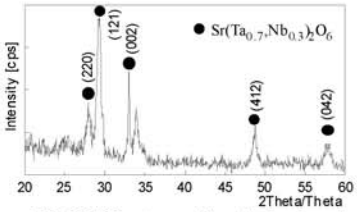

Fig.3 XRD patterns of newly developed $Sr(Ta_{0.7},Nb_{0.3})_2O_6$ on SiO_2/Si formed by the FMLS process.

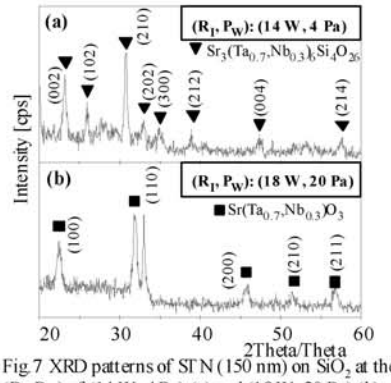

Fig.7 XRD patterns of STN (150 nm) on SiO_2 at the (R_f, P_W) of (14 W, 4 Pa) (a) and (18 W, 20 Pa) (b), respectively.

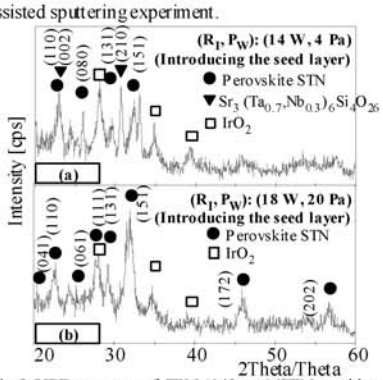

Fig.9 XRD patterns of STN (140 nm)/STN seed layer (10 nm) on SiO_2 at the (R_f, P_W) of (14 W, 4 Pa) (a) and (18 W, 20 Pa) (b), respectively.

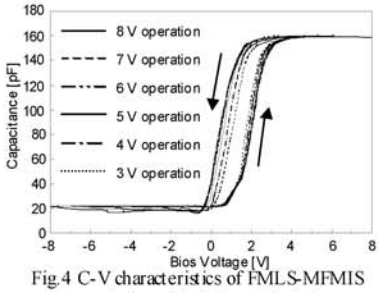

Fig.4 C-V characteristics of FMLS-MFMIS structure device with $Sr(Ta_{0.7},Nb_{0.3})_2O_6$.

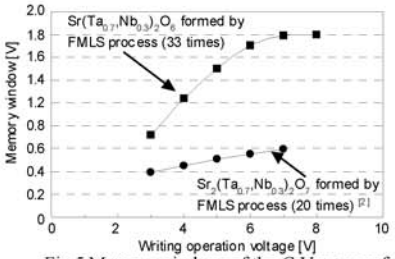

Fig.5 Memory windows of the C-V curves of FMLS-MFMIS devices as function of writing operation voltage.

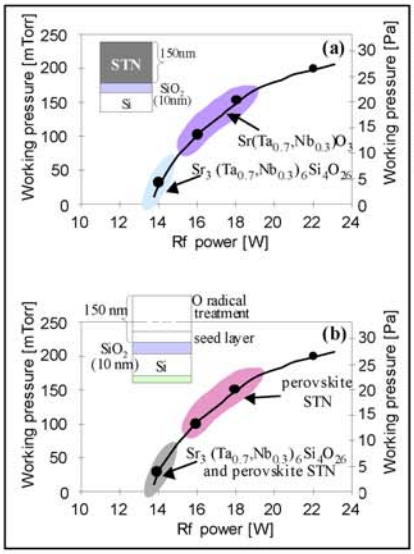

Fig.10 The mapping of the fabricated film phase on the R_f-P_W chart. The substrates are SiO_2/Si (a) and STN seed layer/SiO_2/Si (b), respectively.

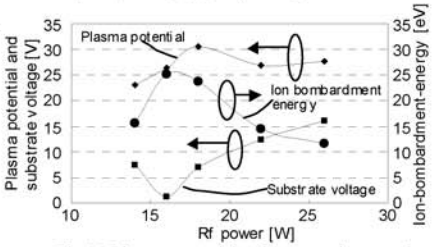

Fig.11 Plasma potential, substrate voltage, and Kr^+ ion-bombardment-energy as function of rf power.

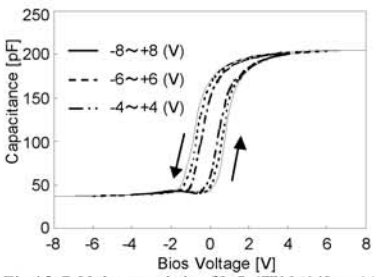

Fig.12 C-V characteristic of IrO_2/STN (140 nm)/STN seed layer (10 nm)/SiO_2/Si device at an (R_f, P_W) of (18 W, 20 Pa).